

Research Article

Open Access



Establishing a biomonitoring baseline by characterizing the hair metabolome across age and sex using high-resolution mass spectrometry

Chih-Wei Chang¹, Chih-Hsing Wu^{2,3,4}, Ru-Hsueh Wang², Yu-Tai Lo^{5,6}, Pao-Chi Liao^{1,7} 

¹Department of environmental and occupational health, National Cheng Kung University, Tainan 704, Taiwan.

²Department of Family Medicine, National Cheng Kung University Hospital, College of Medicine, National Cheng Kung University, Tainan 704, Taiwan.

³Department of Family Medicine, College of Medicine, National Cheng Kung University, Tainan 701, Taiwan.

⁴Institute of Gerontology, College of Medicine, National Cheng Kung University, Tainan 701, Taiwan.

⁵Department of Geriatrics and Gerontology, National Cheng Kung University Hospital, College of Medicine, National Cheng Kung University, Tainan 704, Taiwan.

⁶Department of Public Health, College of Medicine, National Cheng Kung University, Tainan 704, Taiwan.

⁷Department of Food Safety/Hygiene and Risk Management, College of Medicine, National Cheng Kung University, Tainan 701, Taiwan.

Correspondence to: Prof. Pao-Chi Liao, Department of environmental and occupational health, National Cheng Kung University, 138 Sheng Li Road, Tainan 704, Taiwan. E-mail: liaopc@mail.ncku.edu.tw

How to cite this article: Chang CW, Wu CH, Wang RH, Lo YT, Liao PC. Establishing a biomonitoring baseline by characterizing the hair metabolome across age and sex using high-resolution mass spectrometry. *J Environ Expo Assess* 2024;3:19. <https://doi.org/10.20517/jeea.2024.17>

Received: 13 May 2024 **First Decision:** 12 Jul 2024 **Revised:** 12 Aug 2024 **Accepted:** 12 Aug 2024 **Published:** 16 Aug 2024

Academic Editor: Stuart Harrad **Copy Editor:** Dong-Li Li **Production Editor:** Dong-Li Li

Abstract

Hair provides an excellent matrix for long-term biomonitoring due to its chemical accumulation during growth. Despite recent uses of hair for biomonitoring to characterize the chemical exposome across demographics, no established baseline exists for the hair metabolome based on age and sex. This study aimed to establish a baseline for the hair metabolome influenced by age and sex, utilizing an Orbitrap mass spectrometer, a high-resolution mass spectrometry (HRMS) technique. We collected hair samples from 48 participants divided by age and sex into four groups: elderly males, elderly females, young males, and young females. Metabolic profiling was conducted using ultrahigh-performance liquid chromatography coupled with Q Exactive™ Plus Orbitrap mass spectrometer. Our analysis revealed significant age- and sex-dependent variations in metabolite profiles. Volcano plots highlighted the differential metabolic features between groups, with age showing a stronger influence on metabolic variations in females and sex in younger individuals. We identified 205 chemical compounds affected by age and/or sex, with



© The Author(s) 2024. **Open Access** This article is licensed under a Creative Commons Attribution 4.0 International License (<https://creativecommons.org/licenses/by/4.0/>), which permits unrestricted use, sharing, adaptation, distribution and reproduction in any medium or format, for any purpose, even commercially, as long as you give appropriate credit to the original author(s) and the source, provide a link to the Creative Commons license, and indicate if changes were made.



a significant portion showing overlap in their influence. Pathway enrichment analysis pinpointed perturbations in 41 metabolic pathways, including those involved in lipid metabolism, amino acid turnover, and hormone-associated pathways. Notably, the pathways of arachidonic acid metabolism and fatty acid biosynthesis were consistent with known age and sex influences. Our findings underscore the potential of using hair metabolomics for comprehensive environmental exposure assessment and health research, offering insights into the biological impact of age and sex on the human metabolome.

Keywords: Hair, metabolomics, high-resolution mass spectrometry (HRMS), biomonitoring, age- and sex-dependent metabolism

INTRODUCTION

Biomonitoring is an approach used to assess the doses of environmental pollutants to which humans are exposed by measuring either the parent compounds or their corresponding biotransformation products in biospecimens following the absorption of these chemicals into the body^[1,2]. This approach is integral for public health investigations as it provides direct evidence of the actual exposure of individuals to environmental pollutants, rather than estimates based on environmental samples^[2]. A recent study investigated the levels of 59 persistent organic pollutants (POPs) in plasma, finding that p,p'-DDE, HCB, and β -HCH were detected and quantified in more than 95% of the samples^[3]. This underscores the importance of continuous biomonitoring investigations to track these substances within human populations and evaluate the effectiveness of environmental policies. Biomonitoring has been widely applied in evaluating the contamination of ecosystems and assists in the regulatory assessment of chemicals. It is particularly useful in occupational health for monitoring workers' exposure to hazardous substances^[4-6]. In one study, 14 structure-related metabolite signals were quantified in urine samples from five rubber workers using ultra-high-performance liquid chromatography coupled with high-resolution mass spectrometry/mass spectrometry (UHPLC-HRMS/MS)^[6]. Additionally, another recent report revealed the relationship between the levels of naphthalene in the air and those of its exposure markers in urine samples, showing that 1-NMA, 1,2-DHN, 1-and 2-naphthol are suitable exposure for assessing occupational exposure to naphthalene^[7]. Recently, biomonitoring has been extended to include large-scale population assessments, such as the National Report on Human Exposure to Environmental Chemicals in the United States. This survey evaluates chemicals known to have adverse health effects across different demographic groups^[8].

Blood and urine are commonly used as biological samples in biomonitoring studies. According to the National Report on Human Exposure to Environmental Chemicals, hydrophobic parent compounds such as per- and polyfluoroalkyl substances are primarily detected in serum due to their protein-binding properties and poor water solubility^[9]. Although these compounds are less frequently detected in urine, trace amounts can still be found depending on the sensitivity of the analytical methods used. Additionally, the biotransformation products formed when environmental pollutants undergo biotransformation reactions in the human body are more soluble in urine. For instance, phthalate metabolites are commonly used as exposure markers to evaluate phthalate ester exposure in biomonitoring investigations, as the half-life of phthalate esters is approximately 12 h in urine^[10]. Consequently, both blood and urine samples are valuable for biomonitoring investigations. However, the variability in exposure times and the fluctuations in chemical compound levels in these matrices can complicate the profiling of environmental chemical alterations over extended periods^[11-13]. In contrast, hair serves as an excellent matrix for long-term biomonitoring due to the accumulation of chemicals during its growth^[14-16]. A study indicated that hair allows the detection of both parent pesticides and hydrophilic metabolites, while urine can only be applied for hydrophilic chemicals^[17]. Additionally, the exposure markers of phthalate esters could be detected and quantified in rat and human hair samples^[18,19]. Moreover, 28 exposure markers of DPHP were identified in

the hair matrix, whereas only 7 exposure markers of DPHP were detected in the urine 30 days post-exposure in rats^[20]. This disparity underscores the utility of hair for long-term determination of exposure markers in biomonitoring. A 1-cm hair segment typically represents approximately one month of exposure markers and endogenous metabolite accumulation, providing a stable record of exposure^[21,22]. Segmented hair analysis, based on the average growth rate of hair, can offer insights into metabolic changes over time^[21]. Thus, hair provides a broader detection window and a more enduring record of metabolite accumulation compared to blood and urine in biomonitoring investigations.

Hair has recently been utilized for biomonitoring investigations to characterize the chemical exposome across various demographic populations^[23-27]. Variations in the human exposome might be influenced by numerous factors, such as genetics, ethnicity, age, and sex^[28-30]. Among these, age and sex significantly affect hormone levels, enzyme activities, and metabolic rates, which can introduce potential confounding factors when characterizing long-term chemical exposome and conducting biomonitoring investigations. Establishing a baseline associated with age and sex by characterizing hair metabolome is essential for using hair in environmental exposure assessment across different demographic groups. This approach might eliminate the confounding factors related to age and sex in biomonitoring investigations. However, a baseline for the hair metabolome based on age and sex has not yet been established in humans. Metabolomics, an omics approach that focuses on identifying small molecules (< 1,500 Da) in biological systems, has become a suitable strategy for exploring hair metabolome baseline for biomonitoring investigations^[31]. In this study, we aimed to establish a baseline of the metabolic profile in human hair across age and sex using high-resolution mass spectrometry (HRMS).

EXPERIMENTAL

Study design

We aimed to explore the differences of metabolites in human hair based on age and sex using HRMS-based metabolomics approach for developing a baseline for biomonitoring investigation. This study design is shown in [Figure 1](#). This study was divided into three parts: hair collection and preparation, data acquisition and processing, and statistical analysis, identification, distribution, and metabolic pathway search.

In the Hair collection and preparation section, hair samples were collected from a diverse group of 48 volunteers, categorized into four equal groups: old males (OM), old females (OF), young males (YM), and young females (YF). The participants were enlisted from the National Cheng Kung University and its corresponding hospital located in Tainan, Taiwan. Hair metabolites were extracted using procedures established and optimized previously^[32].

In the data acquisition and processing section, the samples including hair extract samples, an instrumental analysis QC sample, sample preparation QC samples, and solvent blank were subjected to UHPLC-HRMS analysis. These were then analyzed using UHPLC-HRMS analysis in full scan mode to obtain the mass spectrometry signals. The reverse phase column was used for hair metabolome profiling. The data were imported into the MS-DIAL for data processing^[33]. The data processing procedure included peak detection and peak alignment.

In statistical analysis, identification, distribution, and metabolic pathway search section, the discriminatory features associated with age and sex were filtered by univariate analysis using Student's *t* test. The discriminatory features were determined by $|\log_2(\text{Fold change})| \geq 1$ with *P* values calculated by *t* test below 0.05. The discriminatory features underwent extra fragmentation analysis to obtain the MS/MS spectrum for chemical identification. For chemical identification, the MS/MS spectral database search is performed

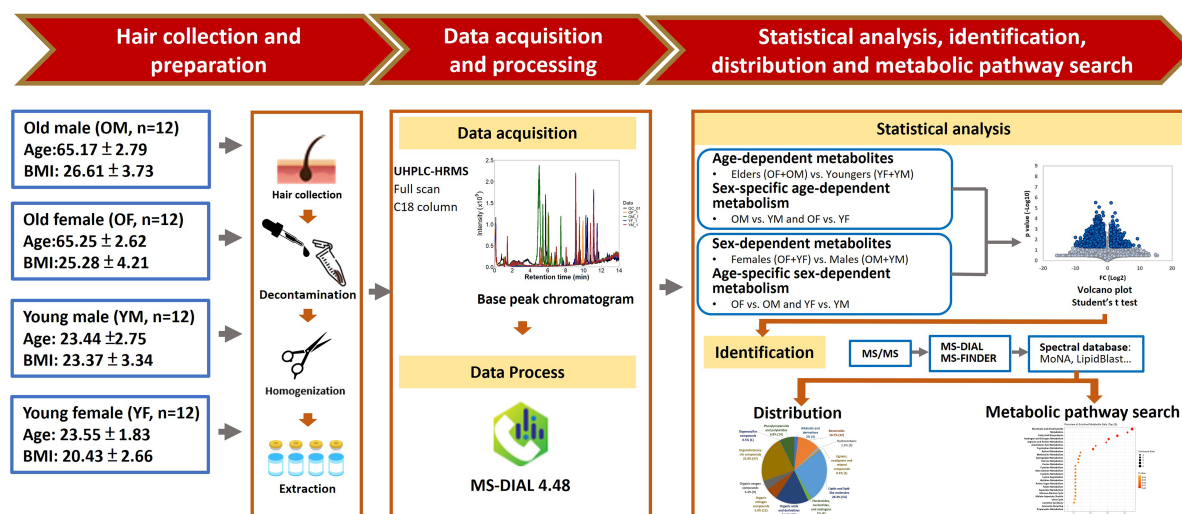


Figure 1. Study design for determining a biomonitoring baseline by characterizing the hair metabolome across age and sex. A study design for exploring the variations of metabolomic profiles with age and sex in human hair by UHPLC-HRMS. Hair samples from the elder group (12 males and 12 females) and the younger group (12 males and 12 females) were collected and subjected to untargeted metabolomics analysis. After hair sample decontamination, homogenization, and extraction, the hair extracts were analyzed with UHPLC-HRMS. The raw MS data were converted to peak lists using MS-DIAL for feature detection, alignment, and compound identification to explore chemical structure, and then, the metabolic pathways were analyzed. UHPLC-HRMS: Ultra-high-performance liquid chromatography coupled with high-resolution mass spectrometry; MS: mass spectrometry.

for identifying chemical compounds according to a previous study^[34]. The MS/MS spectral database was constructed by experimental MS/MS spectrum of reference authentic standards (Massbank of North America) and in silico predicted MS/MS spectrum (MS-FINDER)^[35]. The chemical compounds showing significant alternation across age and sex were subjected to pathway enrichment analysis using MetaboAnalyst 5.0 to discover the metabolic pathways associated with age or sex.

Hair sampling and metabolite extraction

Hairs were cut 0.1 cm away from the scalp with scissors, firm in aluminum foil, and stored at 4 °C until further analysis. Throughout the collection phase, each participant signed a written informed consent form, complying with the protocols established by the Institutional Review Board of National Cheng Kung University Hospital (IRB approval numbers A-ER-107-373 and B-ER-108-188). The washing procedure is a mandatory step to remove contaminants deposited on the hair shaft according to the Hair Testing Association guidelines. Twenty milligrams of hair samples were weighed in a glass tube, washed with acetone (3 mL), and then with deionized water (DIW, 3 mL) in an ultrasonic bath for 2 min each. The wash solution was then discarded, and the samples were dried under nitrogen. Afterward, the dried hair samples were cut into small pieces with a pair of scissors and subjected to the extraction procedure. Six milligrams of washed hair samples were mixed with 300 μ L of methanol: phosphate buffer saline (PBS) 50:50 (v/v) solvent and extracted for 240 min at 55 °C with 37k Hz for ultrasonic-associated extraction. After that, the extracts were centrifuged at 15,000 \times g for 15 min and the supernatants were collected. The hair extract was then evaporated to dryness by SpeedVac (EYELA, cue-2200) and the residue was reconstituted with 50% MeOH (30 μ L). An instrumental quality control (QC) sample for monitoring the robustness of instrumental analysis was prepared by pooling 5 μ L of each of 48 hair extracts, resulting in a total pooled hair extract of approximately 240 μ L. This sample was analyzed after every 4 hair extract injections, with a total of 12 instrumental QC samples analyzed within the analytical sequence [Supplementary Table 1]. Regarding the QC procedure for sample preparation, a pooled QC sample was prepared by combining approximately 10 mg of each of 48 hair samples, resulting in a total pooled sample weighing approximately 480 mg. From this

sample, five replicates of 6 mg each were subjected to the sample preparation procedure described previously. Moreover, to evaluate the levels of noise signals from the extraction solvent, methanol: phosphate buffer saline (PBS) 50:50 (v/v) solvent underwent the same extraction procedure as the hair sample with triplicate.

UHPLC-HRMS analysis

A UHPLC system coupled with a Q Exactive orbitrap mass spectrometer system (Thermo Fisher Scientific) was used for sample analysis. Chromatographic separation was performed on a Waters Acquity UPLC BEH C18 column (2.1 mm × 100 mm, 1.7 μm). The mobile phase consisted of (A) 2% acetonitrile (ACN) in DIW with 0.1% formic acid and (B) 100% ACN with 0.1% formic acid. The gradient conditions were as follows: 0-1 min, 2% B; 1-11 min, 2%-99% B; 11-13 min, 99% B; 13-13.01 min, 99%-2% B; 13.01-14 min, 2% B. The flow rate was set at 0.25 mL/min. Separation using gradient elution at a flow rate of 0.35 mL/min: 0-2 min, 1% of B; 2-2.01 min, 25% of B; 2.01-5 min, 25%-55% of B; 5-14 min, 55%-99% of B; 14-15 min, 99% of B; 15-15.01 min, 25% of B; and 15.01-16 min, 1% of B. The column temperature was maintained at 40 °C and the injection volume was 5 μL. Electrospray ionization was operated in both positive and negative modes. The mass range of *m/z* 100-1,000 was recorded at the resolution of 70,000 in MS₁. The MS/MS operated in data-dependent acquisition (DDA) mode with a targeted mass list adopted for the fragmentation using higher-energy collisional dissociation (HCD), in which normalized collision energies were at 10%, 20%, 50%, and 100%, respectively.

Data processing, statistical analysis, and metabolic pathway enrichment analysis

The raw data collected by HRMS were converted to the “.mzXML” format by MSconverter, and the converted files were further converted into “.abf” format. The converted files were imported into MS-DIAL 4.48^[33] and were processed for feature detection, alignment, and identification. During alignment, the tolerance for retention time was set at 0.2 min and *m/z* value was set at 0.0015 Da. Features with S/N < 3 were considered as the absence of peaks and hence filtered. Each raw abundance value was normalized by dividing it based on the sum of the raw abundance values of all peaks in the corresponding sample before performing a univariate analysis to discover the differential features. Discriminatory features were filtered by $|\log_2(\text{fold-change})| \geq 1$ and $P \leq 0.05$. The discriminatory features were subjected to extra fragmentation analysis for chemical identification. Chemical identification was performed based on the accuracy of precursor mass and tandem mass spectrometry (MS/MS) fragmentation spectral matching using a combination of different tools, including MS-DIAL with MassBank of North America (MoNA) database which was downloaded on 1 June 2023 and MS-FINDER 3.52 with PubChem, Human Metabolome Database (HMDB), and LIPID MAPS as the backend knowledge base. For performing the MS-DIAL with MoNA database, a cutoff value for MS/MS spectral match score was set at 70 (Maximum = 100). For performing MS-FINDER 3.52, a cutoff value of match score was set at 7 (maximum = 10).

The confidence level of metabolite identification was defined using the criteria reported by Schymanski *et al.*^[36]. The chemical structures of the discriminatory features were determined using the MS/MS analysis, but it provided insufficient information for one single exact structure, assigned as a level-3 annotation. Only one chemical structure of the discriminatory features was determined using the MS/MS analysis, assigned as a level-2 annotation. The Classyfire was used to classify the categories of the identified discriminatory chemical compounds based on their chemical structures^[37]. The InChI strings of the chemical compounds were retrieved by the package “webchem” using R 4.4.3. Subsequently, the InChI was imported into Classyfire to obtain the chemical categories. To determine the alterations in metabolic pathways related to age and sex, we used the online software MetaboAnalyst 5.0^[38] to perform pathway enrichment analysis. The metabolites collect the detectable specimen sources using the online database HMDB^[39].

RESULTS AND DISCUSSION

Volcano plots of age- and sex-dependent differential features and identification of differential features

To explore a biomonitoring baseline in human hair across age and sex, we enlisted 48 volunteers divided into two distinct age groups: 61~70 years old (Old group, $N = 24$) and 18~27 years old (Young group, $N = 24$), listed in [Table 1](#). Among the Old group, the mean age was approximately 65 years, with a mean BMI of 25.9. This group was further divided into two subgroups: 12 old females (OF) and 12 old males (OM). There were no statistically significant differences between OF and OM in terms of age ($P = 0.94$), BMI ($P = 0.44$), smoking status ($P = 0.064$), and alcohol consumption ($P = 0.46$). However, cosmetic hair treatment ($P < 0.05$) showed a statistically significant difference between OF and OM, indicating that this factor varies notably by sex within the older age group. Among the Young group, the mean age and BMI were approximately 24 years and 20 kg/m², respectively. This group was also divided into two subgroups: 12 young females (YF) and 12 young males (YM). The characteristics between YF and YM showed no statistically significant differences, indicating that sex did not influence the characteristics within the younger age group.

The samples, including 48 hair extracts, 1 instrumental QC sample, 5 sample preparation QC sample, and 3 blank samples, were analyzed using UHPLC-HRMS in both positive and negative ion modes. For evaluating the analytical reproducibility by instrumental analysis and sample preparation, the principal component analysis (PCA) was performed [[Supplementary Figure 1](#)]. The blue and pink dots in [Supplementary Figure 1](#) represent the 6 injections of instrumental QC sample and 5 replicates of sample preparation QC sample, respectively. It was shown that not only the 6 injections of instrumental QC samples but also 5 sample preparation QC samples were clustered tightly in the plot, indicating that minimal technical errors were presented in instrumental analysis and sample preparation procedure. Significant changes in peak abundance due to age and sex ($|\log_2(\text{fold-change})| \geq 1$ and $P\text{-value} \leq 0.05$) are depicted in volcano plots [[Figures 2 and 3](#)]. In age-dependent features, the positive ion mode showed 1,402 peaks upregulated and 1,228 peaks downregulated [[Figure 2A](#)], while the negative ion mode had 648 peaks upregulated and 230 peaks downregulated [[Figure 2B](#)]. In the positive ion mode, 266 features were upregulated and 589 downregulated in older males compared to young males [[Figure 2C](#)], and 1,812 features upregulated versus 1,306 downregulated in older females compared to young females [[Figure 2E](#)]. In the negative ion mode, 139 features were upregulated and 99 downregulated in older males compared to young males [[Figure 2D](#)], while 734 were upregulated and 388 downregulated in older females compared to young females [[Figure 2F](#)]. For sex-dependent features, 695 features were upregulated and 785 downregulated in the positive ion mode [[Figure 3A](#)], with 127 upregulated and 509 downregulated in the negative ion mode [[Figure 3B](#)]. In the positive ion mode, 330 features were upregulated and 219 downregulated in older females compared to older males, while 798 were upregulated and 1,194 downregulated in young females compared to young males [[Figures 3C and E](#)]. In the negative ion mode, 65 features were upregulated and 214 downregulated in older females compared to older males, with 211 upregulated and 901 downregulated in young females compared to young males [[Figures 3D and F](#)]. The MS feature count is higher in the positive ion mode than in the negative ion mode [[Figures 2 and 3](#)]. Age-dependent features show a greater number of changes in females than in males in both ion modes, indicating a more significant relativity of metabolites with age in females. Similarly, sex-dependent features reveal a greater number of changes in younger individuals than in older ones in both ion modes, indicating higher relativity of metabolites with sex in younger individuals. Overall, these findings suggest that age-dependent features exhibit sex specificity in females and sex-dependent features exhibit age specificity in younger individuals.

The peaks with significant abundance changes were subjected to tandem mass spectrometry (MS/MS) for chemical structure identification. Two hundred and five chemical compounds were identified, with 71 chemical compounds being identified through MS-DIAL with MoNA database and 134 chemical

Table 1. Characteristics of study participants

Characteristic	61-70 years old			P (OM vs. OF)	18-27 years old			P (YM vs. YF)	
	Total	OM	OF		Total	YM	YF		
Age (years, mean ± SD)	65.2 ± 2.8	65.2 ± 2.2	65.3 ± 2.7	0.94	23.5 ± 2.4	23.5 ± 1.9	23.4 ± 2.9	0.92	
BMI (kg/m ² , mean ± SD)	25.9 ± 4.1	26.6 ± 4	25.2 ± 4.4	0.44	21.7 ± 3.4	20.4 ± 2.8	23.4 ± 3.6	0.06	
Cosmetic hair treatment	Never	11	0	< 0.05	22	11	7	0.09	
	Dyeing	11	1		10	0	0		4
	Perming	0	0		0	2	1		1
	Both	2	0		2	0	0		0
Smoking status	Never	21	9	0.06	24	12	12	1.00	
	Current	0	0		0	0	0		
	Past	3	3		0	0	0		0
Alcohol consumption	Never	20	9	0.46	20	9	11	0.27	
	Current	3	2		1	4	3		1
	Past	1	1		0	0	0		0

OM: Old males; OF: old females; YM: young males; YF: young females; SD: standard deviation.

compounds being identified by MS-FINDER with the HMDB, PubChem, and LIPID MAPS databases. These chemical compounds are listed in [Supplementary Table 2](#). Among them, 96 chemical compounds were associated with age, 45 chemical compounds were related to sex, and 64 chemical compounds were linked to both age and sex. This comprehensive set of metabolites defines the baseline metabolic profile for environmental exposure assessment across different demographic groups. The established baseline highlights significant age- and sex-related variations in metabolic profiles, emphasizing the need to consider these demographic factors in biomonitoring studies. This comprehensive baseline serves as a valuable tool for further research, facilitating more accurate assessments of environmental exposure and its potential health impacts.

In recent years, hair has been increasingly used for biomonitoring investigations. Therefore, the 205 baseline compounds identified in hair were compared with those reported in human urine or blood. Using the Human Metabolome Database (HMDB) for comparison, 140 of the 205 baseline compounds are recorded in HMDB^[39]. Among the 140 hair baseline metabolites, 70 of these compounds have been identified in human blood, and 66 of these chemicals have been identified in human urine. A total of 77 of these compounds have previously been detected in urine or blood. This comparison highlighted that the chemical composition in human hair might differ from that in urine or blood. The chemicals were incorporated into human hair matrix and accumulated over extended periods, reflecting long-term chemical exposure and metabolic changes, whereas urine and blood typically represent more immediate metabolic states. These differences underscore the importance of understanding the unique metabolic profiles captured by different biological matrices and the potential implications for biomonitoring and environmental exposure assessments.

Taxonomic distribution of chemical compounds

To elucidate the relationship between sex-dependent and age-dependent compounds among the 205 identified chemicals, a Venn diagram is presented in [Figure 4A](#). Of these, 96 compounds (46.8%) are significantly influenced by age, 45 (22%) by sex, and 64 (31.2%) by both age and sex. The taxonomic distribution of the 205 chemical compounds is categorized into 12 classes based on chemical entities [[Figure 4B](#)]. These classes include lipid and lipid-like molecules (26.3%, 54 compounds), organoheterocyclic compounds (22.9%, 47 compounds), organic acids and derivatives (16.6%, 34 compounds), benzenoids

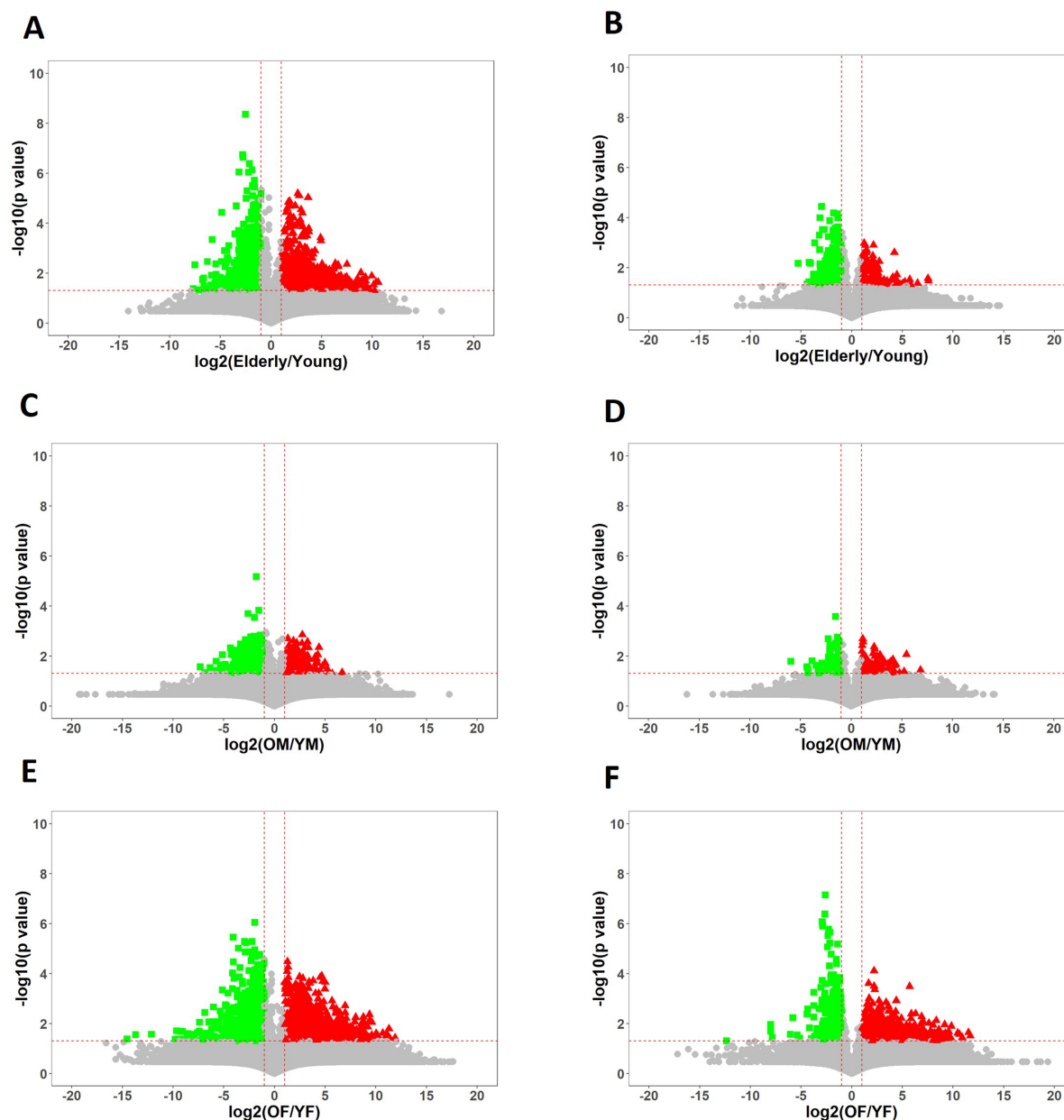


Figure 2. Volcano plots for filtering age-dependent features. Volcano plots illustrated the perturbed features between elders and younger in (A) positive mode and (B) negative ion mode; In addition, the volcano plots show the comparison of OM and YM in (C) positive and (D) negative ion modes, and the comparison of OF and YF in (E) positive and (F) negative ion modes. The dark blue spot represents the features displayed with larger magnitude fold changes (x-axis, $|\log_2(\text{elder/younger})| \geq 1.0$) and statistical significance difference (y-axis, $-\log P\text{-value} \geq 1.33$). (For interpretation of the references to color in this figure legend, the reader is referred to the Web version of this article.) OM: Old males; YM: young males; OF: old females; YF: young females.

(10.7%, 22 compounds), phenylpropanoids and polyketides (6.8%, 14 compounds), organic nitrogen compounds (5.9%, 12 compounds), organic oxygen compounds (2%, 4 compounds), nucleosides, nucleotides, and analogs (2%, 4 compounds), alkaloids and derivatives (1.6%, 4 compounds), hydrocarbons (1.5%, 3 compounds), lignans, neolignans, and related compounds (0.5%, 1 compound), and organosulfur compounds (0.5%, 1 compound). This distribution indicates that both non-polar compounds, such as lipids and lipid-like molecules, as well as polar compounds, like organoheterocyclic compounds and organic acids and derivatives, are detectable in hair metabolism.

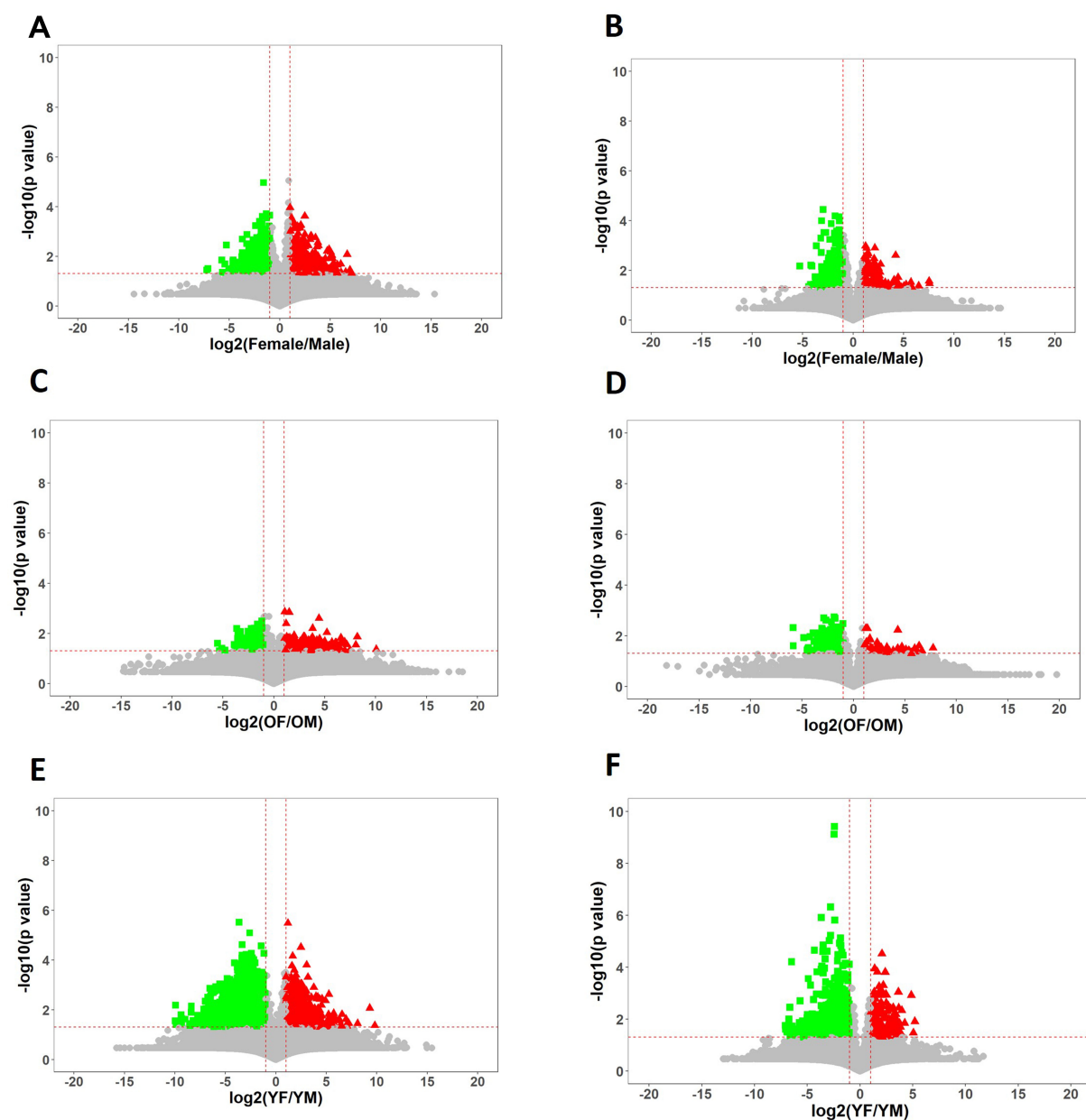


Figure 3. Volcano plots for screening sex-dependent features. Volcano plots illustrated the perturbed features between females and males in (A) positive mode and (B) negative ion mode; In addition, the volcano plots show the comparison of OF and OM in (C) positive and (D) negative ion modes, and the comparison of YF and YM in (E) positive and (F) negative ion modes. The dark blue spot represents the features displayed with larger magnitude fold changes (x -axis, $|\log_2(\text{elder/younger})| \geq 1.0$) and statistical significance difference (y -axis, $-\log P\text{-value} \geq 1.33$). OF: Old females; OM: old males; YF: young females; YM: young males.

To investigate the influence of environmental exposure or diets on metabolites related to age/sex, a total of 9 major metabolites, such as amino acids and lipids and 8 environmental exposure or diet-related chemicals were selected for the correlation analysis [Supplementary Figure 2]. The diethyl phthalate, monobutyl phthalate, and deisopropylatrazine were selected to represent environmental exposure, and alpha-linolenic acid, arachidonic acid, cinnamic acid, equol, and piperettine represented dietary chemicals. The heatmap

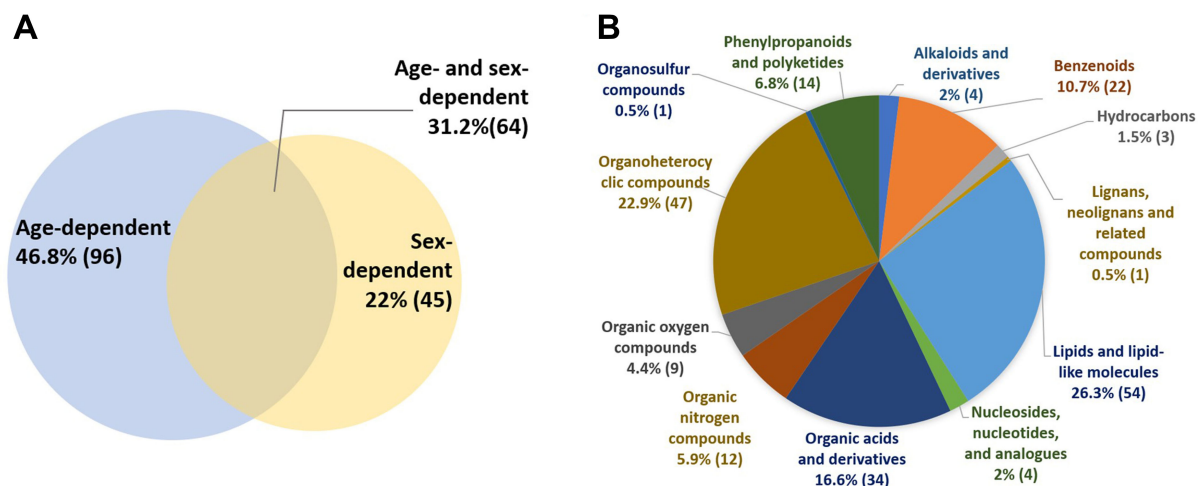


Figure 4. Venn diagram of age- and sex-dependent metabolites and pie chart of compounds classification. (A) The numbers of age-dependent, sex-dependent, and both age- and sex-dependent metabolites are shown in Venn diagram; (B) Taxonomic distribution of chemical compounds was classified and illustrated by pie chart. The numbers of features are indicated in brackets.

demonstrated that most environmental pollutants/ dietary chemicals and the metabolites associated with age/sex do not exhibit a high correlation. Additionally, most correlations are not statistically significant, as indicated by the lack of pronounced color changes. This suggests that the metabolites linked to age and sex may not be directly related to environmental pollution or diet. However, it is important to note that these results are based on partial data. A more comprehensive questionnaire and biomonitoring approach will be implemented in the future to collect detailed exposure data, allowing for a more thorough and comprehensive analysis.

The emerging organic contaminants (EOC) were identified in the human hair, and with significant differences observed based on age or sex. They included the plasticizers (monobutyl phthalate and diethyl phthalate), surfactants (dodecyl hydrogen sulfate and 2-dodecoxyethyl hydrogen sulfate), personal care products (diethylamino hydroxybenzoyl hexyl benzoate), and pesticide (deisopropylatrazine). However, the POPs were not discovered in the hair samples. The potential reason was that our sample preparation procedure might not be suitable for the POPs which were lower hydrophobic chemicals. Our sample preparation procedure involved using methanol and PBS to extract as many chemicals as possible from human hair. POPs such as PFAS, dioxin, and PCB were considered as more hydrophobic chemicals that are hard to solve in the mixture of methanol and PBS. For the analysis of POPs, optimizing a specific sample preparation procedure will be required.

Age- and sex-dependent differential metabolites and perturbed metabolic pathways

To investigate the effects of age- and sex-dependent metabolites in metabolic pathways, pathway enrichment analysis was conducted on 205 compounds using the online tool MetaboAnalyst 5.0^[38] [Figure 5]. This analysis identified 41 perturbed metabolic pathways, detailed in Table 2. These pathways are categorized into eight types: lipid metabolism, amino acid metabolism, carbohydrate metabolism, cofactor and vitamin metabolism, hormone-associated pathways, nucleotide metabolism, biosynthesis of other secondary metabolites, and other metabolic processes [Table 2]. Of the 41 pathways, 13 are age-dependent, 11 are sex-dependent, and 17 are influenced by both age and sex. To determine if the age- and/or sex-related metabolic pathways identified from hair metabolism align with previous findings, a PubMed search was conducted. Out of the 41 pathways, 30 have been reported in prior studies as being age- and/or sex-

Table 2. Age- and sex-dependent metabolic pathways

Pathway classification	Pathway name	Detected METABOLITES IN THIS STUDY	Related to AGE OR SEX IN THIS STUDY	Ref.
Lipid metabolism	Arachidonic acid metabolism	L-glutamic acid, arachidonic acid, leukotriene a4, 8,9-epoxyeicosatrienoic acid, 15-deoxy-d-12,14-PGJ2	Age, sex	[40,41]
	Fatty acid biosynthesis	Biotin, palmitic acid, 3-hydroxybutyric acid, dodecanoic acid, trans-Dodec-2-enoic acid, trans-Tetra-dec-2-enoic acid	Age, sex	[42,43]
	Mitochondrial beta-oxidation of medium chain saturated fatty acids	Dodecanoic acid	Age, sex	-
	Beta oxidation of very long chain fatty acids	Dodecanoic acid	Age, sex	[44]
	Sphingolipid metabolism	Sphinganine	Age	[45]
	Alpha linolenic acid and linoleic acid metabolism	Linoleic acid, arachidonic acid, alpha-linolenic acid, stearidonic acid	Sex	[46,47]
Carbohydrate metabolism	Propanoate metabolism	Biotin, L-glutamic acid	Age, sex	[48]
	Citric acid cycle	Biotin	Sex	[49]
	Gluconeogenesis	Biotin	Sex	[50]
	Pyruvate metabolism	Biotin	Sex	[51]
Amino ACID METABOLISM	Alanine metabolism	Biotin, L-glutamic acid	Age, sex	[50]
	Arginine and proline metabolism	L-glutamic acid, L-proline, ornithine	Age, sex	[52]
	Tryptophan metabolism	L-glutamic acid, kynurenic acid, L-tryptophan, 2-aminobenzoic acid, 3-hydroxyanthranilic acid	Age, sex	[53,54]
	Carnitine synthesis	N6,N6,N6-trimethyl-L-lysine	Age, sex	-
	Tyrosine metabolism	L-glutamic acid	Age	[55]
	Histidine metabolism	L-glutamic acid	Age	-
	Lysine degradation	L-glutamic acid	Age	-
	Methionine metabolism	Dimethylglycine, 2-oxo-4-methylthiobutanoic acid	Age	[56]
	Aspartate metabolism	L-glutamic acid	Age	[57]
	Cysteine metabolism	L-glutamic acid	Age	-
	Malate-aspartate shuttle	L-glutamic acid	Age	[58]
	Beta-alanine metabolism	L-glutamic acid	Age	[59]
	Glutamate metabolism	Biotin, L-glutamic acid	Sex	[60]
	Glutathione metabolism	L-glutamic acid, pyroglutamic acid	Sex	[61]
Valine, leucine and isoleucine degradation	Biotin, L-glutamic acid, L-isoleucine	Sex	-	
Hormone ASSOCIATED METABOLISM	Estrone metabolism	Estradiol	Age, sex	[62]
	Androgen and estrogen metabolism	Estradiol, testosterone glucuronide	Age, sex	[63]
Biosynthesis OF OTHER SECONDARY Metabolism	Caffeine metabolism	5-acetylamino-6-formylamino-3-methyluracil	Age, sex	[64]
Nucleotide metabolism	Purine metabolism	Adenine, L-glutamic acid, hypoxanthine	Age, sex	[62]
Metabolism of COFACTORS AND VITamins	Retinol metabolism	All-trans-13,14-dihydroretinol	Age, sex	[65,66]
	Folate metabolism	L-glutamic acid	Age	[67]
	Nicotinate and nicotinamide metabolism	L-glutamic acid, N1-methyl-2-pyridone-5-carboxamide	Age	[68]
	Biotin metabolism	Biotin	Sex	[69]
Others	Ammonia recycling	Biotin, L-glutamic acid	Age, sex	-
	Phenylacetate metabolism	Alpha-N-phenylacetyl-L-glutamine	Age, sex	[70]
	Urea cycle	L-glutamic acid, ornithine	Age, sex	[71,72]

Threonine and 2-oxobutanoate degradation	Biotin	Sex	-
Glucose-alanine cycle	L-glutamic acid	Age	-
Amino sugar metabolism	L-glutamic acid	Age	-
Transfer of acetyl groups into mitochondria	Biotin	Sex	-
Warburg effect	Biotin, L-glutamic acid	Sex	-

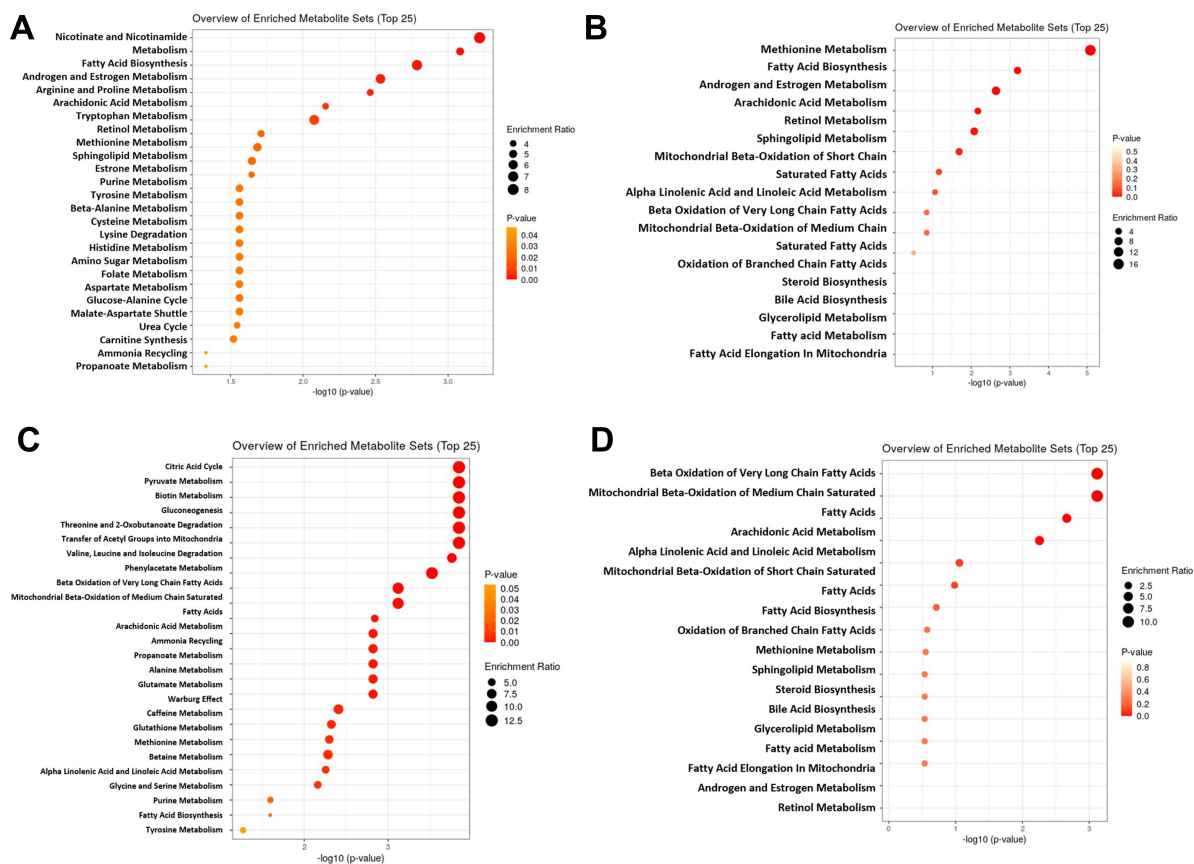


Figure 5. Pathway enrichment analysis for 41 metabolic pathways affected by age and sex. The enriched metabolite sets of (A) age-dependent metabolites, (B) age-dependent lipids, (C) sex-dependent metabolites, and (D) sex-dependent lipids are presented. The enriched metabolite sets in metabolites and lipids are analyzed using the online software MetaboAnalyst 5.0. The x-axis displayed the $-\log_{10}(P)$ value from the enrichment analysis. The size of the circles for each metabolic pathway represented the enrichment ratio, calculated as observed hits divided by expected hits, while their color indicated the p values computed by enrichment analysis.

related, while 11 have not. Fourteen of these 30 pathways align with the age and/or sex associations observed in previous studies, including arachidonic acid metabolism and fatty acid biosynthesis [Table 2].

However, 16 pathways exhibit differences from prior research. For example, propanoate metabolism, which involves the conversion of propionate to propanol adenylate by propionyl-CoA synthase and acetyl-CoA synthase, is linked to both age and sex based on hair metabolism^[73]. Previous studies have identified this pathway as age-related but not sex-related [Table 2]. Biotin metabolism is associated with sex in this study, whereas it has been shown to be age-related in earlier research^[69]. Phenylacetate metabolism is identified as age- and sex-related based on hair metabolism, yet no prior studies have documented this association.

Among the 11 metabolic pathways not reported to be age- and/or sex-related, one involves lipid metabolism, four pertain to amino acid metabolism, and six relate to other metabolic processes. For instance, mitochondrial beta-oxidation of medium-chain saturated fatty acids, categorized under lipid metabolism, is associated with both age and sex in this study, although no prior research has confirmed this. The four amino acid metabolisms - valine, leucine and isoleucine degradation, carnitine synthesis, lysine degradation, and cysteine metabolism - show distinct age or sex associations based on hair metabolism, yet no studies have established these connections. Additionally, other metabolisms like ammonia recycling, glucose-alanine cycle, and amino sugar metabolism show age-related trends, while threonine and 2-oxobutanoate degradation, transfer of acetyl groups into mitochondria, and the Warburg Effect are identified as sex-related, again without prior research confirmation. This analysis demonstrates that hair metabolism can reveal nuanced insights into age- and/or sex-dependent metabolic variations using UHPLC-HRMS. Moreover, the distribution of intensities of the major metabolites, including glutamic acid, biotin, estradiol, and arachidonic acid, within these four groups (OF, OM, YF, and YM) was plotted in [Supplementary Figure 3](#). For glutamic acid, biotin, estradiol, and arachidonic acid, the statistically higher intensity was discovered in the OF group compared to the YF group, indicating that they were associated with age. For glutamic acid and estradiol, the statistically higher intensity was identified in the YM group compared to the YF group, suggesting that they were related to sex.

Limitations

It is significant to discuss some inherent limitations that may affect the interpretation of our findings in this study. First, some of the hair samples collected for this study had undergone cosmetic treatment, which might be a confounding factor for evaluating the altered metabolome across age and sex. For example, Eisenbeiss *et al.* reported that treatment of hair with 9% hydrogen peroxide for 30 min resulted in statistically significant changes in a total of 69 metabolites^[74]. Significant alternations in amino acids, cysteine acid, and lipids in hair were observed during the cosmetic treatments, including perming, dyeing and bleaching^[75]. Although the hair after cosmetic treatments should be ideally excluded from this study, doing so would make it challenging to recruit enough participants. Secondly, 205 chemical compounds included in 41 metabolic pathways were discovered to be associated with age or sex. This set of chemical compounds and metabolic pathways can serve as a baseline for future biomonitoring investigations. However, the precise measurements of the concentrations of these chemicals were not available in this study. Once the precise levels of these chemicals in human hair are determined, it will greatly enhance the use of hair for biomonitoring investigations, providing more valuable information and facilitating its application in environmental exposure assessments. Thirdly, underlying health conditions can significantly influence the metabolome and exposome, potentially confounding the results and interpretations of our study. The absence of this critical information might affect the accuracy and reliability of our findings. Including comprehensive health profiles of participants would help account for the impact of underlying diseases.

CONCLUSION

In this study, we investigate the impact of age and sex on metabolism using hair samples analyzed through UHPLC-HRMS. A total of 41 significant metabolic distinctions across different age and sex groups were identified, thereby contributing valuable insights into the biological impact of these factors on the human metabolome. These results indicated that age has a pronounced influence on metabolic profiles, especially among females, while sex-related metabolic differences are more prominent in younger cohorts. These findings underscore the complexity of metabolic interactions and the importance of considering both age and sex in biomonitoring and health research. A total of 205 distinct chemical compounds were identified, demonstrating the intricate nature of how these factors interplay to affect metabolic pathways. Importantly, our research highlights several key metabolic pathways affected by age and sex, including lipid metabolism and amino acid turnover. Noteworthy are the pathways such as arachidonic acid metabolism and fatty acid

biosynthesis, which consistently exhibit dependencies on both age and sex, reflecting their critical roles in maintaining physiological homeostasis and response to environmental exposures. This study represents a significant step toward establishing a reliable hair metabolomic baseline, which can serve as a robust tool for environmental exposure assessment. This advantage is critical for studies requiring a longitudinal perspective on exposure and metabolic dynamics. As we advance our understanding of the hair metabolome's complexity, we continue to advocate for the integration of metabolomic data with clinical and environmental data to better understand the full scope of exposure and metabolic response. The implications of our findings are manifold, providing a foundation for future investigations and applications in the field of biomonitoring and beyond.

DECLARATIONS

Acknowledgments

The authors gratefully acknowledge the mass spectrometry analysis supported by the National Taiwan University Consortia of Key Technologies and National Taiwan University Instrumentation Center, Taiwan, and ICP00401 and MS004000 equipment belonging to the Core Facility Center of National Cheng Kung University, Taiwan.

Authors' contributions

Conducted the original draft writing and revision, the experiment, data curation and analysis: Chang CW
Responsible for revising the manuscript and recruiting subjects: Wu CH, Wang RH, Lo YT
Designed the study, oversaw its conceptualization and supervision, administered the project, and revised the manuscript: Liao PC

Availability of data and materials

Not applicable.

Financial support and sponsorship

This work was supported by the National Science and Technology Council, Taiwan (grant number MOST109-2113-M-006-015, MOST110-2113-M-006-014, MOST111-2113-M-006-011, and NSTC 112-2113-M-006-002).

Conflicts of interest

Liao PC is an Editorial Board member of *Journal of Environmental Exposure Assessment*, while other authors declared that there are no conflicts of interest.

Ethical approval and consent to participate

Throughout the collection phase, each participant signed a written informed consent form, complying with the protocols established by the Institutional Review Board of National Cheng Kung University Hospital (IRB approval numbers A-ER-107-373 and B-ER-108-188).

Consent for publication

Not applicable.

Copyright

© The Author(s) 2024.

REFERENCES

1. Needham LL. Introduction to biomonitoring. *J Chem Health Saf* 2008;15:5-7. DOI
2. Needham LL, Calafat AM, Barr DB. Uses and issues of biomonitoring. *Int J Hyg Environ Health* 2007;210:229-38. DOI PubMed
3. Henríquez-Hernández LA, Ortiz-Andrelluchi A, Álvarez-Pérez J, et al. Human biomonitoring of persistent organic pollutants in elderly people from the Canary Islands (Spain): a temporal trend analysis from the PREDIMED and PREDIMED-Plus cohorts. *Sci Total Environ* 2021;758:143637. DOI
4. Albertini R, Bird M, Doerr N, et al. The use of biomonitoring data in exposure and human health risk assessments. *Environ Health Perspect* 2006;114:1755-62. DOI PubMed PMC
5. Zhou Q, Zhang J, Fu J, Shi J, Jiang G. Biomonitoring: an appealing tool for assessment of metal pollution in the aquatic ecosystem. *Anal Chim Acta* 2008;606:135-50. DOI
6. Wang Y, Hsu J, Hsu Y, Liao P. Identification of potential urinary exposure markers for the toxicant diisononyl phthalate in rubber worker urine specimens by high-resolution mass spectrometry-based metabolomics. *URINE* 2019;1:8-16. DOI
7. Klotz K, Weiß T, Zobel M, et al. Validity of different biomonitoring parameters in human urine for the assessment of occupational exposure to naphthalene. *Arch Toxicol* 2019;93:2185-95. DOI
8. Crinnion WJ. The CDC fourth national report on human exposure to environmental chemicals: what it tells us about our toxic burden and how it assists environmental medicine physicians. *Altern Med Rev* 2010;15:101-9. PubMed
9. USCDC. Fourth national report on human exposure to environmental chemicals. Updated tables, March 2021 : volume three: analysis of pooled serum samples for select chemicals, NHANES 2005-2016. Available from: <https://stacks.cdc.gov/view/cdc/105344>. [Last accessed on 15 Aug 2024].
10. Hoppin JA, Brock JW, Davis BJ, Baird DD. Reproducibility of urinary phthalate metabolites in first morning urine samples. *Environ Health Perspect* 2002;110:515-8. DOI PubMed PMC
11. Slupsky CM, Rankin KN, Wagner J, et al. Investigations of the effects of gender, diurnal variation, and age in human urinary metabolomic profiles. *Anal Chem* 2007;79:6995-7004. DOI
12. Saude EJ, Adamko D, Rowe BH, Marrie T, Sykes BD. Variation of metabolites in normal human urine. *Metabolomics* 2007;3:439-51. DOI
13. Giskeødegård GF, Davies SK, Revell VL, Keun H, Skene DJ. Diurnal rhythms in the human urine metabolome during sleep and total sleep deprivation. *Sci Rep* 2015;5:14843. DOI PubMed PMC
14. Caplan YH, Goldberger BA. Alternative specimens for workplace drug testing. *J Anal Toxicol* 2001;25:396-9. DOI PubMed
15. Jang WJ, Choi JY, Park B, et al. Hair metabolomics in animal studies and clinical settings. *Molecules* 2019;24:2195. DOI PubMed PMC
16. Alves A, Kucharska A, Erratico C, et al. Human biomonitoring of emerging pollutants through non-invasive matrices: state of the art and future potential. *Anal Bioanal Chem* 2014;406:4063-88. DOI
17. Hardy EM, Dereumeaux C, Guldner L, et al. Hair versus urine for the biomonitoring of pesticide exposure: Results from a pilot cohort study on pregnant women. *Environ Int* 2021;152:106481. DOI
18. Hsu JY, Ho HH, Liao PC. The potential use of diisononyl phthalate metabolites hair as biomarkers to assess long-term exposure demonstrated by a rat model. *Chemosphere* 2015;118:219-28. DOI PubMed
19. Hsu JF, Chang WC, Ho WY, Liao PC. Exploration of long-term exposure markers for phthalate esters in human hair using liquid chromatography-tandem mass spectrometry. *Anal Chim Acta* 2022;1200:339610. DOI PubMed
20. Shih CL, Wu HY, Liao PM, et al. Profiling and comparison of toxicant metabolites in hair and urine using a mass spectrometry-based metabolomic data processing method. *Anal Chim Acta* 2019;1052:84-95. DOI
21. Delplancke TDJ, de Seymour JV, Tong C, et al. Analysis of sequential hair segments reflects changes in the metabolome across the trimesters of pregnancy. *Sci Rep* 2018;8:36. DOI PubMed PMC
22. Henderson GL. Mechanisms of drug incorporation into hair. *Forensic Sci Int* 1993;63:19-29. DOI PubMed
23. Iglesias-González A, Schweitzer M, Palazzi P, et al. Investigating children's chemical exposome - Description and possible determinants of exposure in the region of Luxembourg based on hair analysis. *Environ Int* 2022;165:107342. DOI PubMed
24. Chang CW, Hsu JY, Su YH, Chen YC, Hsiao PZ, Liao PC. Monitoring long-term chemical exposome by characterizing the hair metabolome using a high-resolution mass spectrometry-based suspect screening approach. *Chemosphere* 2023;332:138864. DOI PubMed
25. Ruiz-Castell M, Le Coroller G, Pexaras A, et al. Characterizing the adult exposome in men and women from the general population: Results from the EHES-LUX study. *Environ Int* 2023;173:107780. DOI
26. Gilles L, Govarts E, Rodriguez Martin L, et al. Harmonization of human biomonitoring studies in Europe: characteristics of the HBM4EU-aligned studies participants. *Int J Environ Res Public Health* 2022;19:6787. DOI PubMed PMC
27. Polledri E, Mercadante R, Consonni D, Fustinoni S. Cumulative pesticides exposure of children and their parents living near vineyards by hair analysis. *Int J Environ Res Public Health* 2021;18:3723. DOI PubMed PMC
28. Bucher ML, Anderson FL, Lai Y, Dicent J, Miller GW, Zota AR. Exposomics as a tool to investigate differences in health and disease by sex and gender. *Exposome* 2023;3:osad003. DOI PubMed PMC
29. Ding E, Wang Y, Liu J, Tang S, Shi X. A review on the application of the exposome paradigm to unveil the environmental determinants of age-related diseases. *Hum Genomics* 2022;16:54. DOI PubMed PMC
30. Costanzo M, Caterino M, Sotgiu G, Ruoppolo M, Franconi F, Campesi I. Sex differences in the human metabolome. *Biol Sex Differ*

- 2022;13:30. [DOI](#) [PubMed](#) [PMC](#)
31. Muthubharathi BC, Gowripriya T, Balamurugan K. Metabolomics: small molecules that matter more. *Mol Omics* 2021;17:210-29. [DOI](#) [PubMed](#)
 32. Chang WC, Wang PH, Chang CW, Chen YC, Liao PC. Extraction strategies for tackling complete hair metabolome using LC-HRMS-based analysis. *Talanta* 2021;223:121708. [DOI](#) [PubMed](#)
 33. Tsugawa H, Cajka T, Kind T, et al. MS-DIAL: data-independent MS/MS deconvolution for comprehensive metabolome analysis. *Nat Methods* 2015;12:523-6. [DOI](#) [PubMed](#) [PMC](#)
 34. Kind T, Tsugawa H, Cajka T, et al. Identification of small molecules using accurate mass MS/MS search. *Mass Spectrom Rev* 2018;37:513-32. [DOI](#) [PubMed](#) [PMC](#)
 35. Tsugawa H, Kind T, Nakabayashi R, et al. Hydrogen rearrangement rules: computational MS/MS fragmentation and structure elucidation using MS-FINDER software. *Anal Chem* 2016;88:7946-58. [DOI](#) [PubMed](#) [PMC](#)
 36. Schymanski EL, Jeon J, Gulde R, et al. Identifying small molecules via high resolution mass spectrometry: communicating confidence. *Environ Sci Technol* 2014;48:2097-8. [DOI](#)
 37. Djoumbou Feunang Y, Eisner R, Knox C, et al. ClassyFire: automated chemical classification with a comprehensive, computable taxonomy. *J Cheminform* 2016;8:61. [DOI](#) [PubMed](#) [PMC](#)
 38. Pang Z, Chong J, Zhou G, et al. MetaboAnalyst 5.0: narrowing the gap between raw spectra and functional insights. *Nucleic Acids Res* 2021;49:W388-96. [DOI](#) [PubMed](#) [PMC](#)
 39. Wishart DS, Guo A, Oler E, et al. HMDB 5.0: the human metabolome database for 2022. *Nucleic Acids Res* 2022;50:D622-31. [DOI](#) [PubMed](#) [PMC](#)
 40. Thomas MH, Pelleieux S, Vitale N, Olivier JL. Dietary arachidonic acid as a risk factor for age-associated neurodegenerative diseases: potential mechanisms. *Biochimie* 2016;130:168-77. [DOI](#) [PubMed](#)
 41. Former F, Kumar C, Luber CA, Fromme T, Klingenspor M, Mann M. Proteome differences between brown and white fat mitochondria reveal specialized metabolic functions. *Cell Metab* 2009;10:324-35. [DOI](#)
 42. Corona-Meraz FI, Vázquez-Del Mercado M, Ortega FJ, Ruiz-Quezada SL, Guzmán-Ornelas MO, Navarro-Hernández RE. Ageing influences the relationship of circulating miR-33a and miR-33b levels with insulin resistance and adiposity. *Diab Vasc Dis Res* 2019;16:244-53. [DOI](#) [PubMed](#)
 43. Sibbons CM, Brenna JT, Lawrence P, et al. Effect of sex hormones on n-3 polyunsaturated fatty acid biosynthesis in HepG2 cells and in human primary hepatocytes. *Prostaglandins Leukot Essent Fatty Acids* 2014;90:47-54. [DOI](#) [PubMed](#) [PMC](#)
 44. Yang L, Zhang Y, Wang S, Zhang W, Shi R. Decreased liver peroxisomal β -oxidation accompanied by changes in brain fatty acid composition in aged rats. *Neurol Sci* 2014;35:289-93. [DOI](#)
 45. Muilwijk M, Callender N, Goorden S, Vaz FM, van Valkengoed IGM. Sex differences in the association of sphingolipids with age in Dutch and South-Asian Surinamese living in Amsterdam, the Netherlands. *Biol Sex Differ* 2021;12:13. [DOI](#) [PubMed](#) [PMC](#)
 46. Hrelia S, Bordoni A, Celadon M, Turchetto E, Biagi PL, Rossi CA. Age-related changes in linoleate and alpha-linolenate desaturation by rat liver microsomes. *Biochem Biophys Res Commun* 1989;163:348-55. [DOI](#) [PubMed](#)
 47. Burdge GC, Calder PC. Dietary alpha-linolenic acid and health-related outcomes: a metabolic perspective. *Nutr Res Rev* 2006;19:26-52. [DOI](#) [PubMed](#)
 48. Vignoli A, Tenori L, Luchinat C, Saccenti E. Age and sex effects on plasma metabolite association networks in healthy subjects. *J Proteome Res* 2018;17:97-107. [DOI](#) [PubMed](#)
 49. Yarian CS, Toroser D, Sohal RS. Aconitase is the main functional target of aging in the citric acid cycle of kidney mitochondria from mice. *Mech Ageing Dev* 2006;127:79-84. [DOI](#) [PubMed](#) [PMC](#)
 50. Snell K, Walker DG. Age-related changes in gluconeogenesis and the metabolism of alanine in the perfused liver of neonatal rats. *Biochem Soc Trans* 1975;3:128-9. [DOI](#)
 51. Agostini A, Yuchun D, Li B, Kendall DA, Pardon MC. Sex-specific hippocampal metabolic signatures at the onset of systemic inflammation with lipopolysaccharide in the APPswe/PS1dE9 mouse model of Alzheimer's disease. *Brain Behav Immun* 2020;83:87-111. [DOI](#) [PubMed](#) [PMC](#)
 52. Xie K, Qin Q, Long Z, et al. High-throughput metabolomics for discovering potential biomarkers and identifying metabolic mechanisms in aging and Alzheimer's disease. *Front Cell Dev Biol* 2021;9:602887. [DOI](#) [PubMed](#) [PMC](#)
 53. van der Goot AT, Nollen EA. Tryptophan metabolism: entering the field of aging and age-related pathologies. *Trends Mol Med* 2013;19:336-44. [DOI](#) [PubMed](#)
 54. Songtachalet T, Roomruangwong C, Carvalho AF, Bourin M, Maes M. Anxiety disorders: sex differences in serotonin and tryptophan metabolism. *Curr Top Med Chem* 2018;18:1704-15. [DOI](#) [PubMed](#)
 55. Durani LW, Hamezah HS, Ibrahim NF, et al. Age-related changes in the metabolic profiles of rat hippocampus, medial prefrontal cortex and striatum. *Biochem Biophys Res Commun* 2017;493:1356-63. [DOI](#)
 56. Stadtman ER, Van Remmen H, Richardson A, Wehr NB, Levine RL. Methionine oxidation and aging. *Biochim Biophys Acta* 2005;1703:135-40. [DOI](#) [PubMed](#)
 57. Luo HH, Feng XF, Yang XL, Hou RQ, Fang ZZ. Interactive effects of asparagine and aspartate homeostasis with sex and age for the risk of type 2 diabetes risk. *Biol Sex Differ* 2020;11:58. [DOI](#) [PubMed](#) [PMC](#)
 58. Goyary D, Sharma R. Late onset of dietary restriction reverses age-related decline of malate-aspartate shuttle enzymes in the liver and kidney of mice. *Biogerontology* 2008;9:11-8. [DOI](#) [PubMed](#)

59. Saransaari P, Oja SS. Characterization of sodium-independent beta-alanine binding to cerebral cortical membranes from 7-day-old and adult mice. *Int J Dev Neurosci* 1994;12:491-7. [DOI](#) [PubMed](#)
60. Taskiran D, Sagduyu A, Yüceyar N, Kutay FZ, Pöğün S. Increased cerebrospinal fluid and serum nitrite and nitrate levels in amyotrophic lateral sclerosis. *Int J Neurosci* 2000;101:65-72. [DOI](#) [PubMed](#)
61. Zhu H, Wang N, Yao L, et al. Moderate UV exposure enhances learning and memory by promoting a novel glutamate biosynthetic pathway in the brain. *Cell* 2018;173:1716-27.e17. [DOI](#)
62. Wehner G, Schweikert HU. Estrone sulfate source of estrone and estradiol formation in isolated human hair roots: identification of a pathway linked to hair growth phase and subject to site-, gender-, and age-related modulations. *J Clin Endocrinol Metab* 2014;99:1393-9. [DOI](#) [PubMed](#)
63. Stanhewicz AE, Wenner MM, Stachenfeld NS. Sex differences in endothelial function important to vascular health and overall cardiovascular disease risk across the lifespan. *Am J Physiol Heart Circ Physiol* 2018;315:H1569-88. [DOI](#) [PubMed](#) [PMC](#)
64. Murray A, Tharmalingam S, Nguyen P, Tai TC. Untargeted metabolomics reveals sex-specific differences in lipid metabolism of adult rats exposed to dexamethasone in utero. *Sci Rep* 2021;11:20342. [DOI](#) [PubMed](#) [PMC](#)
65. Zhang PP, Ma KX, Ke XF, et al. Development and validation of a five-RNA-based signature and identification of candidate drugs for neuroblastoma. *Front Genet* 2021;12:685646. [DOI](#) [PubMed](#) [PMC](#)
66. Li H, Rong Z, Wang H, et al. Proteomic analysis revealed common, unique and systemic signatures in gender-dependent hepatocarcinogenesis. *Biol Sex Differ* 2020;11:46. [DOI](#) [PubMed](#) [PMC](#)
67. Auley MT, Mooney KM, Salcedo-Sora JE. Computational modelling folate metabolism and DNA methylation: implications for understanding health and ageing. *Brief Bioinform* 2018;19:303-17. [DOI](#) [PubMed](#)
68. Liu X, Zhang M, Liu X, et al. Investigation of plasma metabolic and lipidomic characteristics of a chinese cohort and a pilot study of renal cell carcinoma biomarker. *Front Oncol* 2020;10:1507. [DOI](#) [PubMed](#) [PMC](#)
69. Fukuwatari T, Wada H, Shibata K. Age-related alterations of B-group vitamin contents in urine, blood and liver from rats. *J Nutr Sci Vitaminol* 2008;54:357-62. [DOI](#) [PubMed](#)
70. Caterino M, Ruoppolo M, Villani GRD, et al. Influence of sex on urinary organic acids: a cross-sectional study in children. *Int J Mol Sci* 2020;21:582. [DOI](#) [PubMed](#) [PMC](#)
71. Plubell DL, Wilmarth PA, Zhao Y, et al. Extended multiplexing of tandem mass tags (TMT) labeling reveals age and high fat diet specific proteome changes in mouse epididymal adipose tissue. *Mol Cell Proteomics* 2017;16:873-90. [DOI](#) [PubMed](#) [PMC](#)
72. Leskanicova A, Chovancova O, Babincak M, et al. Sexual dimorphism in energy metabolism of wistar rats using data analysis. *Molecules* 2020;25:2353. [DOI](#) [PubMed](#) [PMC](#)
73. Pronk JT, van der Linden-Beuman A, Verduyn C, Scheffers WA, van Dijken JP. Propionate metabolism in *Saccharomyces cerevisiae*: implications for the metabolon hypothesis. *Microbiology* 1994;140:717-22. [DOI](#) [PubMed](#)
74. Eisenbeiss L, Binz TM, Baumgartner MR, Kraemer T, Steuer AE. Cheating on forensic hair testing? Detection of potential biomarkers for cosmetically altered hair samples using untargeted hair metabolomics. *Analyst* 2020;145:6586-99. [DOI](#) [PubMed](#)
75. Joo KM, Kim AR, Kim SN, et al. Metabolomic analysis of amino acids and lipids in human hair altered by dyeing, perming and bleaching. *Exp Dermatol* 2016;25:729-31. [DOI](#)